Miniaturized UWB Bandpass Filters Integrated with Notch Filters Using a Silicon-based Integrated Passive Device Technology

Zhengzheng Wu, Yonghyun Shim, and Mina Rais-Zadeh

EECS Department, University of Michigan, Ann Arbor, MI, 48109, USA

***Abstract* — This paper reports on the implementation of miniaturized UWB filters with low loss, steep rejection, and spurious-free response on a silicon substrate. A UWB filter is demonstrated with an insertion loss of less than 1 dB, 3 dB bandwidth of 7.25 GHz, attenuation of more than 30 dB in both the lower (10 MHz–2.6 GHz) and the upper (12 GHz–20 GHz) stop-bands, occupying only 2.9 mm × 2.4 mm of die area. In addition, a novel design is proposed for the implementation of a narrowband notch filter, which can be integrated with UWB bandpass filters for rejecting strong in-band interferences. A UWB filter integrated with a notch filter is presented having a total footprint of 4.6 mm × 2.9 mm. The notch filter centered at 5.285 GHz provides a maximum attenuation of 23 dB with 10 dB fractional bandwidth of 7% to reject WLAN/WiMAX interferences. The temperature stability of the notch filter is better than 0.4 % in the temperature range of -30 °C to 70 °C.**

***Index Terms* — Bandpass filters, inductive coupling, IPD, lumped passives, MEMS filters, notch filters, UWB.**

I. Introduction

Ultra-wideband (UWB) is an emerging radio technology that enables low power, large bandwidth communication, robust against multipath fading as well as jamming. Since the Federal Communications Commission (FCC) approved the unlicensed use of the frequency spectrum from 3.1 GHz to 10.6 GHz for UWB communication, there has been an increasing interest in utilizing this band specifically for high data rate (up to 500 Mb/s) signal transmission. However, one of the main limitations of UWB communication has been the existence of strong, in-band interferences that can saturate the receiver front-end. This calls for integration of narrow-band interference rejection filters with the UWB bandpass filters. There have been a few reports on the implementation of UWB bandpass filters integrated with narrow-band notch filters based on microstrip, co-planar waveguide, or quasi-lumped components on low-loss microwave substrates such as FR4, or LTCC [1]. While excellent performances have been reported, there is still room for improvement in terms of size miniaturization. In addition, there has been no demonstration of UWB filters on silicon substrates.

In this paper, high-performance and miniaturized UWB bandpass filters integrated with notch filters are demonstrated. The UWB filters are implemented in a silicon-based integrated passive device (IPD) technology platform which offers higher level of integration compared to other low-loss microwave substrates used in prior work. The filters demonstrated in this paper occupy significantly smaller die area (by a factor of at least three) compared to the state-of-the-art UWB filters while offering a competitive performance [1]. In addition, these filters do not require backside metallization, and they are less sensitive to variations in the thickness of the substrate as well as the packaging layer. This later is achieved by designing the filters using co-planar lumped components with proximate ground plane, so that the electro-magnetic field is confined on the surface of the substrate. The presented filter technology is therefore suitable for flip-chip assembly or multi-chip-module (MCM) integration, making the implementation of highly integrated UWB RF front-end modules realizable. This paper discusses the techniques used for mitigating the problems associated with the microwave loss of the silicon substrate as well as the methods used to miniaturize lumped filters on silicon.

II. Filter Integration in a SI-based Integraed Passive Device (IPD) Platform

The UWB filters are fabricated using a silicon-based IPD technology. The fabrication process flow is shown in Fig. 1.

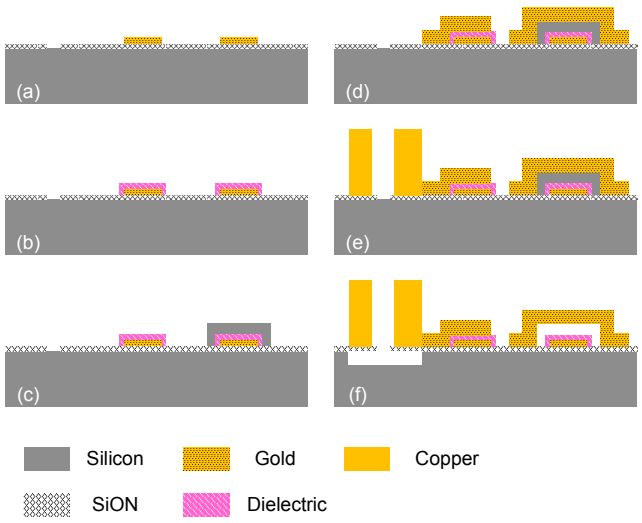

Fig. 1. Process flow of the thin film IPD technology.

The process starts with the deposition of a 2μm-thick low-stress silicon oxynitride dielectric layer on a high-resistivity (> 1 k ·cm) silicon substrate. The processing steps are (a) deposition and patterning of gold as the bottom electrode; (b) deposition of a dielectric layer for metal-insulator-metal (MIM) capacitors; (c) sputtering and patterning amorphous

silicon as a sacrificial layer; (d) gold electroplating for the top metal electrode of MIM capacitors; (e) thick copper electroplating to form high-*Q* inductive components; (f) xenon difluoride gaseous etching of the amorphous silicon to form air-gap cross-bridge, and selectively removing the silicon substrate to reduce the substrate loss. It is worth mentioning that the developed IPD process offers simultaneous fabrication of tunable RF MEMS components. As an example, a tunable capacitor can be fabricated using the deposited gold layer as the bottom electrode, the electroplated gold layer as the top movable membrane, and amorphous silicon as the sacrificial layer, as is demonstrated in [2].

III. DESIGN OF UWB FILTERS

Two different configurations are used for the implementation of filters: (A) UWB elliptic filters, and (B) cascaded lowpass-highpass filters with integrated notch. A new design is utilized for implementing the miniaturized notch filter for rejection of a strong narrow-band interference, which will be discussed in Section III(B).

A. Elliptic Ultra-Wideband Bandpass Filter

Compared to other types of passive filters, elliptic filters require fewer components to provide a sharp roll-off. A fifth-order elliptic filter is used to ensure 30 dB attenuation in both lower (< 2 GHz) and upper (12.5 – 15 GHz) stopbands. Fig. 2(a) illustrates the circuit and the 3D model of the filter used in the HFSS EM simulations. When implemented on a silicon substrate, the parasitics of the substrate distort the frequency response and degrade the filter performance. In the proposed IPD process, silicon is selectively removed beneath the inductors, leaving them firmly supported on a low-loss dielectric membrane and resulting in small substrate parasitics.

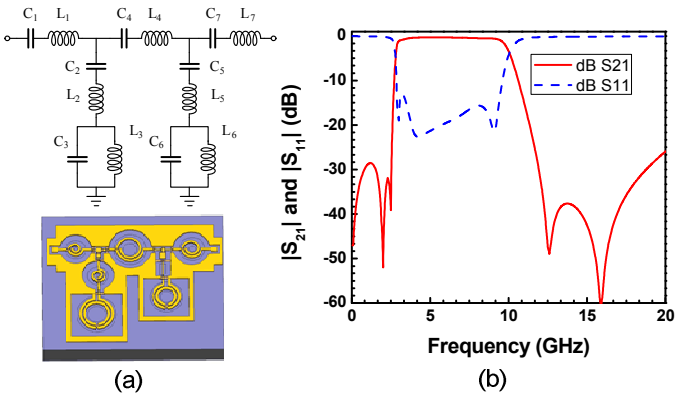

Fig. 2. (a) Circuit schematic and 3D model of the elliptic bandpass filter (overall size: 2.9 mm × 2.4 mm). (b) Fullwave frequency response of the elliptic bandpass filter obtained using HFSS.

In HFSS simulations, the conductivity of electroplated copper is taken as 4.9×10^7 S/m and the substrate loss tangent and conductivity are assumed to be 0.004, and 1 KΩ·cm, respectively. Using these values, the minimum insertion loss of the filter is 0.4 dB and the return loss is better than 15 dB within the passband (2.9 – 9.4 GHz), as shown in Fig. 2(b). The attenuation in the stopbands (< 2.5 GHz and 12–15 GHz) is better than 30 dB. The size of the filter is 2.9 mm× 2.4 mm.

B. Cascaded UWB Bandpass Filter with an Embedded Notch Filter

The second type of bandpass filter is based on generalized Chebyshev configuration, providing better group delay than elliptic network with competitive shape factor. A highpass section is cascaded with a lowpass section to define the UWB bandpass response. Fig. 3(a) shows the circuit diagram of the highpass filter. The inductive T-junction is transformed into a pair of coupled inter-winded inductors for the purpose of size miniaturization. The coupling is further adjusted to generate a transmission zero closer to the passband in order to provide a steep rejection with minimum use of components. The inter-winded coupled pair is optimized for achieving coupling coefficient of 0.2. Using this design, the size of the filter can be reduced to 2.9 mm × 2.4 mm. The lowpass filter circuit is shown in Fig. 3(b), where inductive coupling between L_2 and L_3 controls the transmission zero and the roll-off at the high frequency cut-off region. The parasitic capacitances of the silicon substrate are absorbed into C_1, C_2 and C_3, making it possible to achieve a low-loss filter even on a solid silicon substrate. The 3D model of the cascaded filter is shown in Fig. 4(a). The HFSS simulated response of the cascaded UWB filter on silicon is compared with that of a filter on a micromachined substrate in Fig. 4(b).

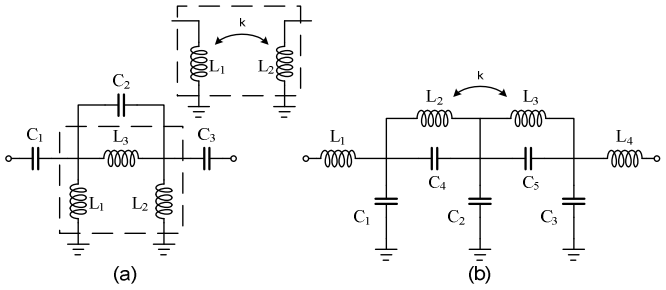

Fig. 3. (a) High pass filter circuit, and (b) lowpass filter circuit.

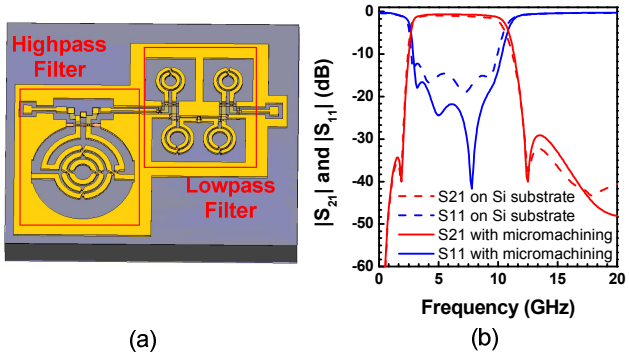

Fig. 4. (a) 3D model of the cascaded bandpass filter (size: 2.9 mm × 2.4 mm). (b) Simulated frequency response of the cascaded UWB filter; dashed lines: on silicon substrate and solid lines: when silicon is removed beneath the inductors.

As is shown in Fig. 4(b), the bandpass filter on micromachined substrate shows a very low insertion loss of 0.7 dB at 6.85 GHz, with return loss of better than 15 dB from 3.1 – 9.9 GHz. The attenuation level in both lower (< 2 GHz) and upper (12.5 – 20 GHz) stopbands is more than 30 dB. The bandpass filter on high-resistivity silicon shows only slightly higher insertion loss of 1 dB, and return loss of better than 13 dB within the passband.

A fixed-frequency notch filter is integrated with the cascaded bandpass filter for rejecting known interferences. The coupled transmission line bandstop filter design [3] is adopted for the notch filter. Lumped components are used to model the transmission line [4], as shown in the circuit diagram of Fig. 5. Using this technique narrow band notch filters can be designed using low-value inductors. Low-value inductors are favorable as they not only occupy smaller area but also can be designed to have higher *Q*s. In this work, a second-order notch filter is designed to reject typical narrowband interferences around the 5 GHz wireless local-area network (WLAN). The notch filter design offers size miniaturization, high rejection level of more than 20 dB, and small out-of-band loss. The simulated response of the bandpass filter with the embedded notch is shown in Fig. 6(a). The loss of the filter is less than 1.5 dB at both the lower and the upper passbands. The notch filter centered at 5.25 GHz exhibits a -10 dB bandwidth of 6.3%. The size of the UWB with notch filter is 4.6 mm × 2.9 mm, (Fig. 6(b)).

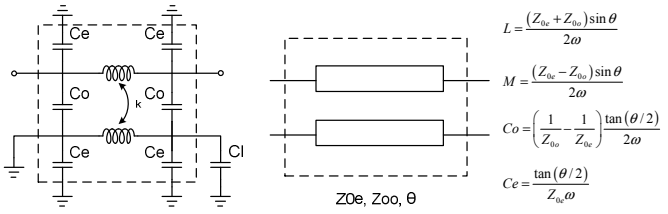

Fig. 5. Circuit implementation of the notch filter.

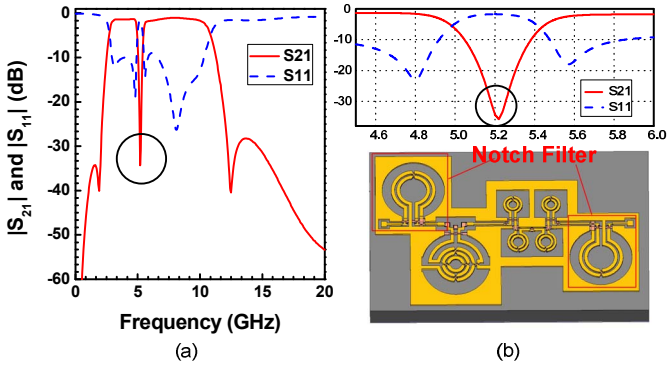

Fig. 6. (a) Simulated frequency response of the UWB bandpass filter with notch. (b) 3D model of the filter (size: 4.6 mm × 2.9 mm).

IV. MEASUREMENT RESULTS

Fig. 7 shows SEM views of the fabricated filters. On-wafer measurement of devices is carried out using an Agilent 8364B network analyzer and Cascade Microtech GSG ACP-probes.

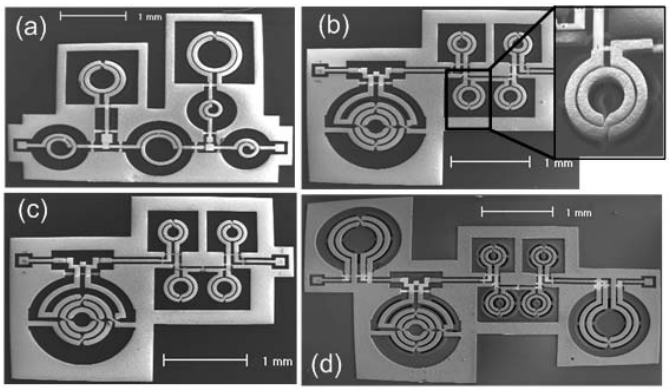

Fig. 7. SEM images of the fabricated UWB filters. (a) Elliptic bandpass filter; (b) cascaded bandpass filter on micromachined silicon substrate; (c) cascaded bandpass filter (without notch) on silicon; and (d) cascaded bandpass filter with notch.

The measured frequency response of the elliptic bandpass filter is shown in Fig. 8. The measured mid-band insertion loss is 1 dB (at 6.85 GHz) and the minimum attenuation is 30 dB at stopbands (<2.6 GHz and 12.5 –20 GHz). This filter exhibits a return loss of more than 15 dB from 3.1 to 9.6 GHz and 3 dB bandwidth of 7.25 GHz. The measured group delay of the filter is shown in Fig. 8(b). As shown, the in-band group delay is less than 0.25 ns. The group delay is extracted using the formula proposed in [5].

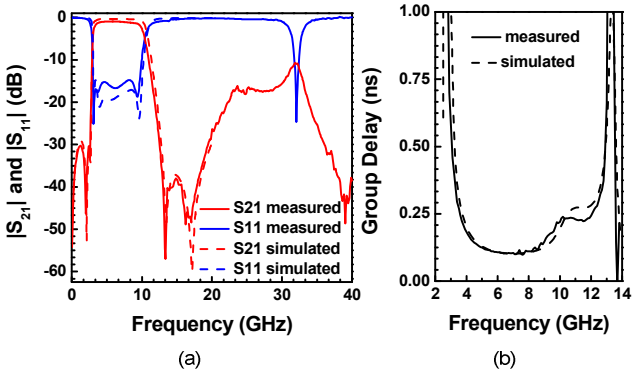

Fig. 8. Measured filter response of the elliptic bandpass filter. (a) Insertion loss and return loss; (b) group delay.

Figs. 9 and 10 show the measured response of the cascaded UWB bandpass on micromachined silicon substrate and on solid silicon substrate, respectively. The cascaded bandpass filter on micromachined substrate has a bandwidth of 7.6 GHz (3–10.6 GHz) within which the return loss is better than 15 dB. The mid-band insertion loss of the filter is 1.1 dB (at 6.85 GHz). This filter exhibits an excellent out-of-band rejection of at least 30 dB at lower (< 2 GHz) and upper (> 13 GHz) sides of the passband with a spurious-free response up to 40 GHz (Fig. 9 (a)). On the other hand, the 3 dB bandwidth of the cascaded bandpass filter on a solid silicon substrate is 7.3 GHz (2.9 –12 GHz). The minimum insertion loss is 1.4 dB, which is slightly higher than the filter on the micromachined silicon substrate. The in-band return loss is also slightly degraded to 11 dB within the passband. The attenuation at

lower (<2 GHz) and upper (> 12.5 GHz) sides of the passband is better than 30 dB. The group delay of both filters (on silicon and on micromachined substrate) is less than 0.25 ns.

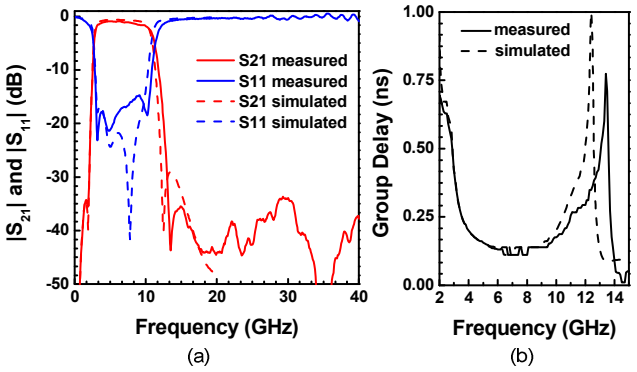

Fig. 9. Measured response of the cascaded bandpass filter on a micromachined silicon substrate (silicon is removed beneath the inductors). (a) Insertion loss and return loss; (b) group delay.

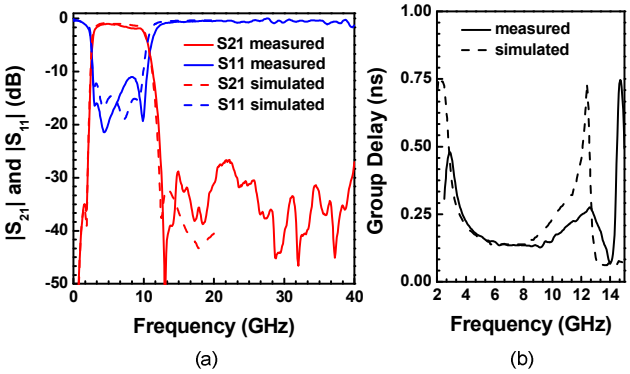

Fig. 10. Measured response of the cascaded bandpass filter on a solid silicon substrate. (a) Insertion loss and return loss; (b) group delay.

The measured response of the bandpass filter with embedded notch filter is plotted in Fig. 11. The minimum insertion loss of the filter in the lower and upper passbands is less than 1.9 dB and 2 dB, respectively. At the notch center frequency of 5.285 GHz, the attenuation is more than 23 dB. The -10 dB fractional bandwidth is 7%. The overall group delay in the passband is within 0.3 ns.

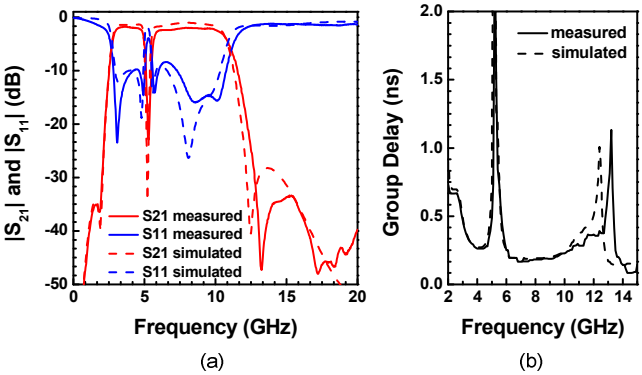

Fig. 11. Measured response of the bandpass filter with embedded notch filter. (a) Insertion loss and return loss; (b) group delay.

As shown in Figs. 8 to 11, the measured responses are in good agreement with the simulations. The slight performance deviation between the measured and simulated responses is due to fabrication inaccuracies.

To study the thermal stability of the micromachined filter, the frequency response of an embedded notch filter (centered at 5.285 GHz at room temp.) is measured from to -30 °C to 70 °C. The filter is temperature stable and the frequency of the notch changes only by 0.4% (or in other words by 40 ppm/°C) under temperature variations, as shown in Fig. 12.

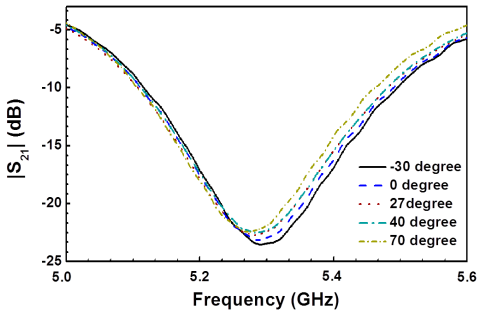

Fig. 12. Notch filter response at difference temperatures.

V. CONCLUSION

In this paper, design and characterization of several UWB filters were discussed. The filters exhibit a low loss on a silicon substrate, which makes them suitable candidates for highly integrated RF front-end modules.

ACKNOWLEDGEMENT

The authors would like to acknowledge the staff of the Lurie Nanofabrication Facility at the University of Michigan for their assistance with fabrication, and Mehrnoosh Vahidpour, and Roozbeh Tabrizian for their help with measurements.

REFERENCES

[1] Z. C. Hao, and J. S. Hong, "Ultrawideband filter technologies," *IEEE Microw. Mag.,* vol.11, no.4, pp.56-68, June 2010.

[2] Y. Shim, Z. Wu, and M. Rais-Zadeh, "A high-performance, temperature-stable, continuously tuned MEMS capacitor," *IEEE MEMS 2011*, Cancun, Mexico, pp. 752-755.

[3] H. C. Bell, "L-resonator bandstop filters," *IEEE Trans. Microw. Theory Tech.,* pp. 2669-2672, Dec 1996.

[4] J. Hogerheiden, M. Ciminera, and G. Jue, "Improved planar spiral transformer theory applied to a miniature lumped element quadrature hybrid," *IEEE Trans. Microw. Theory Tech.,* vol.45, pp.543-545, 1997.

[5] I. Shapir, "Suggestion for a new formula to calculate group-delay from frequency domain measurements," *36th European Microwave Conf.*, pp.1233-1236, Sept. 2006.